3D Joint Inversion of MMT and MCSEM data

Jéssica Larissa da Silva Pinheiro [1], Marcos Welby Correa Silva[1], Anderson Almeida da Piedade[2] and Cícero Roberto Teixeira Régis[1], [1]Graduate Program in Geophysics – UFPA, [2]UFOPA

Abstract

Joint inversion is a mathematical technique in which we use more than one geophysical method to perform the inversion, so the entire data set's processing is done at once using all available information on the physical properties obtained by each method. We apply this technique to the MMT and MCSEM data sets simultaneously and then compare with the inversions for each data separately. These two methods provide complementary information, while MMT provides information about deep structures. MCSEM identifies thin resistive bodies, sharing the same receivers that can collect both datasets. The inversion method used was the Gauss-Newton method with the Marquardt strategy to mitigate computational expenditure. To introduce a priori information, we apply the global smoothness and total variation regularization. We analyzed singular values to measure the amount of data; each method contributes to the solution. We tested the effectiveness of our joint inversion technique using a complex marine model wich represents a layer and a salt dome and another body symbolizing a hydrocarbon reservoir. The results were satisfactory, where we can see the potential of each method. The main information that MMT and MCSEM provide is capable of generating an estimate with greater accuracy in the data than each technique separately, mitigating ambiguities. However, the greatest difficulty encountered was the high computational cost, particularly in constructing the sensitivity matrix.

Introduction

Geophysical inversion is a practice that aims to extract information from geophysical data and thus be able to infer about a geological environment from the physical properties associated with that environment. Each investigation method that can be used in inversion has its limitations and because of that we can use more than one method to eliminate the ambiguities of a problem and thereby we cover these intrinsic limitations and place more emphasis on the potential of each method (Bortolozo, 2016).

Several authors have used more than one geophysical method to perform inversion (Zhang and Li, 2019; Crepaldi et al., 2015; Mackie et al., 2007, Heincke et al., 2006). They call this technique of joint inversion, where the processing of the entire data set is done simultaneously, taking into account all available information on the physical properties obtained by each method. The joint inversion is attractive, because it makes it more controlled with less human intervention and introduces a greater amount of data in the process (Wiik et al., 2013).

In this work, two methodologies were used to implement the joint inversion in electromagnetic data and we applied this process to a problem of hydrocarbon exploration in the marine environment. The first is the Marine Controlled Source Electromagnetic Method (MCSEM) and the second is the Marine Magnetotelluric Method (MMT). MMT is not sensitive to thin layers that have greater resistivity than the medium, as is the case of hydrocarbon reservoirs in thin layers of sediments, however this method can reach great depths of investigation (Simpson and Bahr, 2005). MCSEM is very sensitive to these layers, so it is an important method in the exploration of hydrocarbons in the sea (Mackie et al., 2007; Andréis and Mcgregor, 2008).

According to Abubakar et al. (2011), these two methods have complementary characteristics. Another advantage of using these two methods is data acquisition, considering MMT and CSEM data can be collected in the same survey. MMT data is collected when the MCSEM transmitter is turned off or out of range (Constable and Weiss, 2006). The joint inversion of these two data sets becomes less complex, because they share the same physical parameter: the electrical resistivity (Vozoff and Jupp, 1975).

Some authors have already proven the advantages that the joint inversion of MCSEM and MMT data can provide. Among these works, we can cite Mackie et al. (2007), which used the nonlinear conjugate gradient method to minimize the objective function to simultaneously invert the two data sets, thus managing to more accurately recover the resistive body geometry. Another work developed is from Commer and Newman (2009), where the author uses a hybrid approach in which he proposes a cell-based inversion on a particular area of interest related to a parametric inversion on a regional scale. This approach provided a less ambiguous interpretation of the data measured in hydrocarbon prospecting. Gribenko and Zhdanov (2011) also proposed a joint inversion of MMT and MCSEM 3D data. The inversion method used was the regularized weighted conjugate gradient, in addition to having a technique that limits the range of the receivers, this drastically reduces the computational memory used.

The works mentioned above took advantage of the potential of each method. In the joint inversion, the limitations and ambiguities were reduced, showing good results in the mapping of salt, hydrocarbon and hydrocarbon bodies close to salt bodies. In addition, it proved to be a very useful tool to verify the consistency of the data related to the results of inversion and interpretation obtained from the independent or sequential use of other methods. On the other hand, one of the main difficulties in carrying out the joint inversion is in

choosing the weights that will balance the MCSEM and MMT data.

The objective of this work is to perform the 3D joint inversion of MMT and MCSEM data. This approach aims to contribute to a better delimitation of hydrocarbon reservoirs and a less ambiguous interpretation of the measured data, and with that, we hope to reduce the exploratory risks in prospecting for oil and gas.

In this work, before perform inversion, we used the singular value decomposition (SVD) in order to characterize the effectiveness of the inversion. The Gauss-Newton method was applied with the Marquardt strategy and making use of the global smoothness and total variation regularization ones to perform the joint inversion. To calculate the objective function, the finite element method was used in the frequency domain in unstructured meshes of tetrahedral elements. One difficulty encountered was the high computational cost of the inversion process, especially the large computational time spent in building the sensitivity matrix.

3D modeling of MMT and MCSEM data

The modeling of MCSEM and MMT was performed using the nodal finite element method with tetrahedral elements to solve the problem. The unstructured 3D meshes of tetrahedral finite elements were generated using the TetGen software.

The mathematical details of the modeling of the MCSEM are described in da Silva (2018). The author used a numerical technique to find an approximate solution to the problem. This technique is summarized in using the magnetic vector and scalar electric potentials instead of the electromagnetic fields to obtain the system of differential equations and partial derivatives, where he applied the finite element method. MCSEM uses a horizontal electric dipole (HED) as source. The electromagnetic fields were obtained through numerical derivatives. In this work, we use MCSEM to isotropic case, whose algorithm was developed by da Silva (2018).

As for the mathematical formulation of 3D MMT, we follow the development proposed by Rijo (2004). In the elaboration of the MMT direct problem, the author analytically calculated the primary electric field through the plane wave formulation. The secondary electromagnetic field is described in terms of the magnetic vector and electric scalar potentials solved numerically by the finite element method. The algorithm used for 3D MMT modeling was developed by the researchers in the PRETROBRAS project (Silva and Régis, 2017).

The MMT and MCSEM inversion algorithm was developed by da Piedade (2020). the details will be described next.

SVD Analysis

One step that can be taken before obtaining the inversion solution is the analysis of singular values, obtained by decomposing a matrix into its singular values. The SVD (Singular Value Decomposition) is widely used to decompose a matrix into several matrices that have very important characteristics from the original matrix. Using this decomposition, we going to characterize the effectiveness of the inversion.

Being $\mathbf{A} \in \mathbb{R}^{m \times n}$ a rectangular sensitivity matrix, we can decompose it as follows $\mathbf{A} = \mathbf{USV}^T$, where U is a square matrix of dimension m whose columns provide the eigenvectors associated with $\mathbf{AA}^t$., V is a square matrix, but of dimension n in which its columns show eigenvectors associated with $\mathbf{A}^t\mathbf{A}$ and S is the matrix whose dimension is the same as A where the main diagonal contains the singular value σ (square root of the eigenvalues) of A ordered in decreasing order (σ1 ≥ σ2 ≥ σ3 ≥ ::: ≥ σn). The increase in the dimensions of A implies an increase in the amount of very small singular values (Hansen, 2005).

In this work, the graph of singular values of the Hessian matrix will be shown, because with it we will have the same quantity of singular value for each method since the number of parameters will be the same.

Joint Inversion

The geophysical inverse problem is an ill-posed problem, as it does not meet at least one of the following conditions: existence, uniqueness and stability (Zhdanov, 2002). That is, for a problem to be well-posed, the solution must exist and be unique and in addition, small variations in the data should not cause large variations in the solution. One way to turn a ill-posed problem into a well-posed problem is to introduce a priori information (Silva et al., 2001). This kind of information is introduced using mathematical regularization, as described below.

We use the Gauss-Newton method. It is summarized in that the adjusting functional is approximated by a linear function, so that derivatives of an order greater than 1 are null. That is, the functional adjuster that was initially nonlinear was approximated at **p** by a linear function (Mojabi and Lovetri, 2009). This method mitigates the disadvantage of computational cost for the evaluation of the second derivative matrix (Hessian matrix) of the objective function, as this Hessian is approximated by the multiplication of two Jacobians (first derivative matrix) (Aster et al., 2018). If the minimization of the functional is well approximated by a quadratic form, we reach the minimum sought.

The observed data ($\mathbf{d}^o$) can be described using a nonlinear vector function **F**(p) which is a function of a set of geophysical parameters. Therefore, we assume that:

$$\mathbf{d}^o \approx \mathbf{F}(\mathbf{p}). \quad (1)$$

The objective is to find the set **p** that best approximates the equation (1), so for the joint inversion the functional adjuster between the data is defined by the equations below:

$$\phi_{MT} = \| \mathbf{W}_{MT}(\mathbf{d}^o_{MT} - \mathbf{F}_{MT}(\mathbf{p})) \|^2; \quad (2)$$

$$\phi_{CS} = \| \mathbf{W}_{CS}(\mathbf{d}^o_{CS} - \mathbf{F}_{CS}(\mathbf{p})) \|^2, \quad (3)$$

such that $\mathbf{d}^o_{MT}$ is the MMT observation vector and $\mathbf{F}_{MT}(\mathbf{p})$ is the vector function that describes the estimates of the MMT data and $\mathbf{d}^o_{CS}$ is the vector of MCSEM observations and $\mathbf{F}_{CS}(\mathbf{p})$ is the vector function that describes the estimates of MCSEM data.

The $\mathbf{W}_{MT}$ and $\mathbf{W}_{CS}$ are diagonal weighting matrix used to balance the difference between the dynamic ranges of the MMT and MCSEM and defines the degree of influence of the corresponding data during the joint inversion. The components of the weighting matrix are usually based upon the inverse of the standard deviations of the measurements (Commer and Newman, 2009).

This establishes the problem of finding such p that it minimizes the equations 2 and 3, but this problem is ill-posed. To transform it into a well-posed, mathematical regularization (which will be better discussed later) defined by $\phi_r(\mathbf{p})$, which insert a priori information in relation to the parameters p that you want to estimate. In other words, solving this problem means minimizing the functional called objective function, defined by the expression:

$$\phi_\alpha(\mathbf{p}) = \phi_{MT}(\mathbf{p}) + \phi_{CS}(\mathbf{p}) + \mu\phi_r(\mathbf{p}), \quad (4)$$

where μ is the Lagrange multiplier, which is a regularization parameter responsible for controlling the importance of the a priori information inserted.

We use the Marquardt method to guarantee the convergence, where the step can be controlled through an interactive process. This technique aims to ensure that the estimate of a step is always given in the downward direction of the objective function gradient. To control the step, a positive scalar λ (Marquardt parameter) is added to the diagonal of the resulting Hessian matrix.

The final equation that estimates the parameter is:

$$\Delta\mathbf{p} = -(2\mathbf{A}^T\mathbf{A} + 2\mathbf{B}^T\mathbf{B} + \mu\mathbf{H}_r + \lambda\mathbf{I})^{-1}(2\mathbf{A}^T\mathbf{W}_{MT}(\mathbf{d}^o_{MT} - \mathbf{F}(\mathbf{p})) + 2\mathbf{B}^T\mathbf{W}_{CS}(\mathbf{d}^o_{CS} - \mathbf{F}(\mathbf{p})) - \mu\mathbf{g}_r). \quad (5)$$

As stated earlier, regularization is responsible for transforming an ill-posed problem into a well-posed problem, that is, solving problems of lack of stability and uniqueness. This is done by introducing *a priori* information, which imposes restrictions on the parameters to be estimated, so we try to estimate a set of parameters that adjust the observed data and satisfy these restrictions (Oliveira Jr and Uieda, 2014). *A priori* information can be of a mathematical or geological character. In this work, two types of regularization were applied: Global Smoothness and Total Variation.

The Global Smoothness Estimator restricts the adjacent parameters to obtain values closer to each other, this means that there should be no sudden variations between the adjacent parameters, or that the difference between these parameters must be minimal. The Total Variation regularization, unlike the Global Smoothness regularization, when there is some discontinuity between spatially adjacent parameters, it allows abrupt changes in the parameters. However, the restriction that this regularization imposes is the same as the Global Smoothness.

Result and discussions

The following results were performed in order to test the methodology of joint inversion of MMT and MCSEM data and to prove its effectiveness.

We use synthetic data from a interpretive model that seek to resemble reality to generate the results that will be presented. The synthetic model will be built in order to test the advantages and disadvantages of the methods used (MCSEM and MMT). The first tests will be performed with each method separately and, later, we will apply the joint inversion and compare the results. All tests were performed on Silix machines with 12 cores with an Intel CORE I7-8700 processor, 3.2 GHz and 64 GB of RAM.

In this experiment, we are presenting a greater number of observations and parameters. We use a 3D model with a tetrahedron element generated by the Tetgen software, representing a marine environment. The Figure 1 shows us the geological model we will try to recover with the inversion, where the air has a resistivity of 1012 Ωm, the water layer has resistivity of 0:33 Ωm, the first layer of sedimentary rock has a resistivity of 5 Ωm, a second layer simulating a salt layer has resistivity of 1000 Ωm and the last layer has 20 Ωm of resistivity. This model also has a body of 100 m thick (with a lateral extension of 5 km in the x and y directions), symbolizing a hydrocarbon reservoir. The Figure 2 represent the inversion mesh generated by software Tetgen, where we can observe the interpretation region. The inversion grid is a rectangular block with dimensions 12 km in x, 7 km in y and z 2.5 km. This block is divided into 6000 homogeneous cells, where each represents a parameter. There are 20 cells in the x direction, 20 cells in the y direction and 15 cells in the z direction that increase with depth.

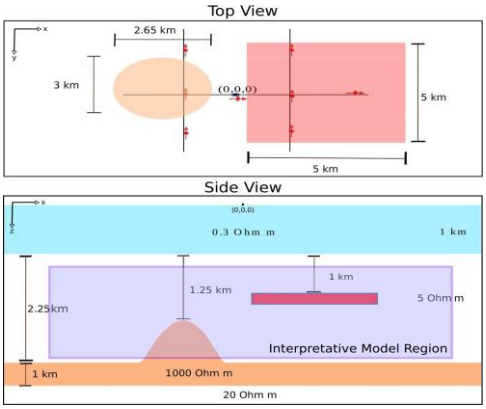

***Figure 1** – Representation of the proposed geological model.*

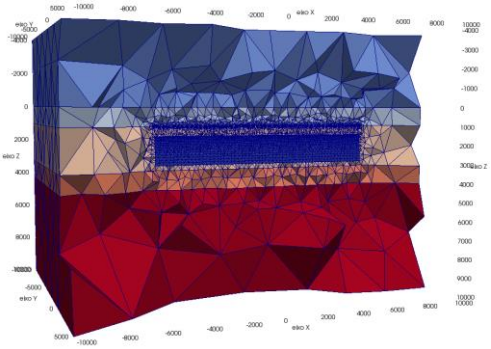

***Figure 2** - Representation of the tetrahedral finite element mesh used to generate the data with 6000 parameters.*

The data acquisition simulations with the MCSEM method were carried out on 3 parallel lines (in y equal to -3 km, 0 and 3 km) with 6 receivers each spaced at 2 km on the x axis starting at x equal to -4 km. It was performed at four measurement frequencies: 0.25 Hz, 0.5 Hz, 0.75 Hz and 1 Hz with inline geometry. We obtained amplitude and phase observations of the electric field for the MCSEM. For the MMT method, we use 40 frequencies between 10^{-3} Hz and 1 Hz to obtain observations of apparent resistivity and phase.

The analysis made next it will be in relation to the size of the null space of the Hessian matrix of each methodology. The null space measurement was performed using the singular values of the Hessian matrix. Figure 3 shows us the graph of the singular values obtained through the SVD, the black curve represents the singular values of the Hessian matrix of the MMT, the magenta curve represents the singular values of the Hessian matrix of the MCSEM and finally the blue curve are the singular values of the Hessian matrix of the joint method. The following graph only shows values above 10^{-8}, because below that, these values will not interfere with our analysis since they are extremely small.

It appears that the null space of the joint methodology is smaller compared to the other methodologies, this means that the problem in question is potentially more stable. Another important point to be highlighted when observing the null space is the information that is introduced when we add another method to do the joint analysis, the addition of this information leads us to believe that the estimate of the parameters at the end of a joint inversion will present a better result if compared to inversions separately.

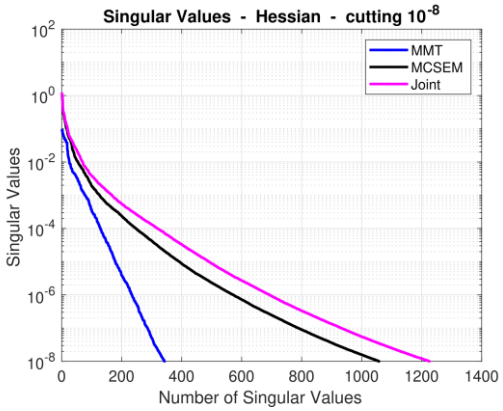

Figure 2 *- Graph of singular values above 10^{-8} of the Hessian matrix of the MMT, MCSEM and the joint method.*

Global Smoothness Regularization - Next, the result of the inversions of MMT and MCSEM data will be presented using only the global smoothness regularization. The process of reversing MMT data using the global smoothness regularization took about 100 hours and made use of 50 GB of RAM. The figure 4 represent the xz plane of the inversion grid. We can observe in this figure, that the method is able to identify the resistive elevation in depth, but it cannot identify the thin body. Also, we were unable to satisfactorily recover the resistivity of the elevation.

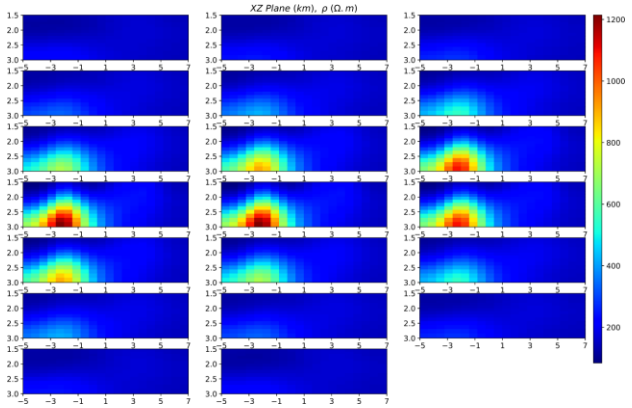

Figure 3 *- Slices of the XZ plane of the model estimated by the inversion of MMT data with the global smoothness regularization.*

The figure 5 show the result of the MCSEM data inversion and represent the xz plane of the estimated model, in that order. When analyzing this figure, we observed that the inversion was able to recover the thin body, which was predicted about the MCSEM method. However, the estimated resistivity slightly exceeded the true resistivity. The processing of this data set took about 75 hours and used 55 GB of RAM.

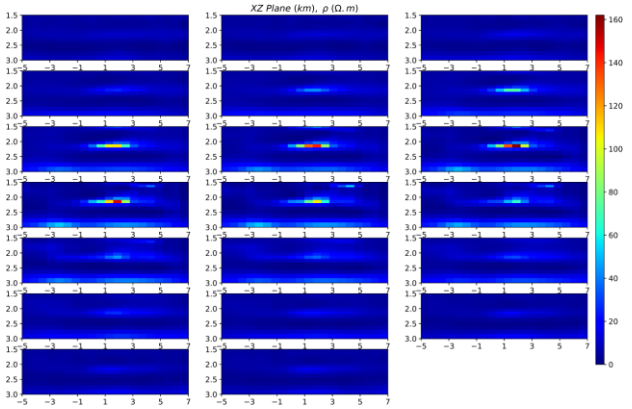

Figure 4 *- Slices of the XZ plane of the model estimated by the inversion of MCSEM data with the global smoothness regularization.*

Next, we have the joint inversion of the MMT and MCSEM methods using the global smoothness regularization. The figure 6 show us the xz plane of the estimated model. As we can see in the following figure, the information that the MCSEM data adds in the joint inversion is greater than that of the MMT data (as was also seen by the graph of singular values). In this way, we can clearly identify the slim body, but with low border delimitation. The elevation is not so clear, due to the estimated resistivity model. This inversion used approximately 55 GB of RAM.

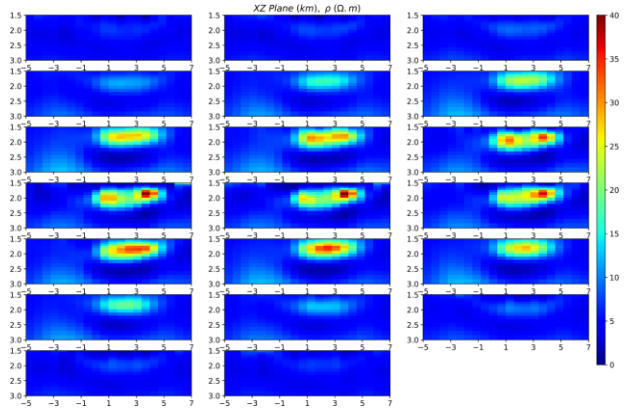

Figure 5 *- Slices of the XZ plane of the model estimated by the joint inversion of the data with the global smoothness regularization.*

In the next figures, we observe the adjustment of the curves, shown from the comparison between the observed data and the data estimated by the joint inversion using the global smoothness regularization. The figure 7 show the MCSEM data for the frequency of 0.25 Hz and for receiver 3, in which the black curve is the observed data and the blue curve is the estimated data. The figure 8 show MMT data for receiver 3, where the red curve represents the observed data and the blue curve the estimated data. These figures show that the data estimated by the joint inversion using the global smoothness regularization adjusted satisfactorily to the observed data.

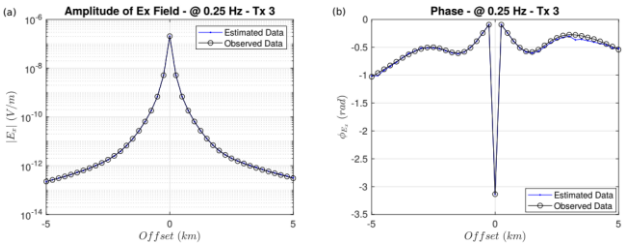

Figure 7 *- Graph of comparison between observed (black curve) and estimated (blue curve) MCSEM data of transmitter 3 for the frequency of 0.25 Hz. (a) Amplitude of the electric field; (b) Phase of the electric field using global smoothness regularization.*

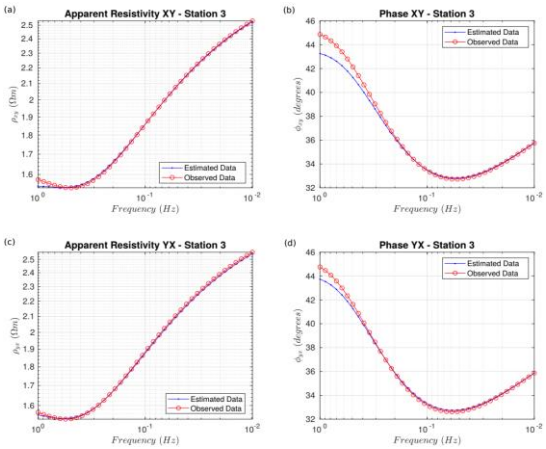

Figure 8 - *Graph of comparison between observed (red curve) and estimated (blue curve) MMT data of the receiver 3. (a) Apparent resistivity XY; (b) Phase XY; (c) Apparent resistivity YX; (d) Phase YX using global smoothness regularization.*

Total Variation Regularization - Finally, we have the results of joint inversion of the MMT and MCSEM methods using the total variation regularization. The figure 9 shows the xz plane of the estimated model. In the figure cited for the total variation regularization, we note a better delimitation of the bodies, due to the imposition of the regularization in relation to the abrupt variations in resistivity. At this point, the total variation was better. This inversion used approximately 55 GB of RAM.

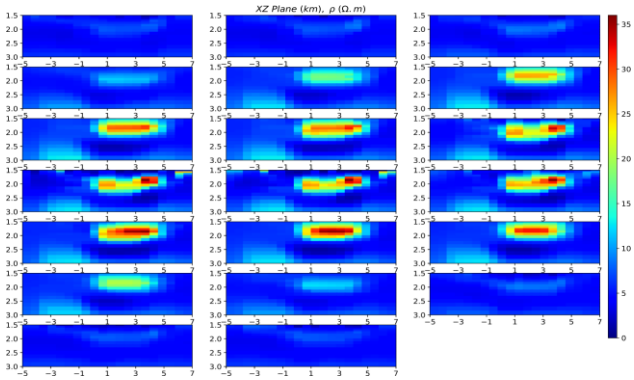

Figure 6 *- Slices of the XZ plane of the model estimated by the joint inversion of the data with the total variation regularization.*

The figures below show the comparison between the observed data and the data estimated by the joint inversion. Thus, we observe the adjustment of the curves. The figure 10 show the MCSEM data for the frequency of 0.25 Hz and for receiver 3, in which the black curve is the observed data and the blue curve is the estimated data. The figure 11 show the MMT data for receiver 3, where the red curve represents the observed data and the blue curve the estimated data. With these figures we observed that the data estimated by the joint inversion using the total variation regularization, adjusted satisfactorily to the observed data.

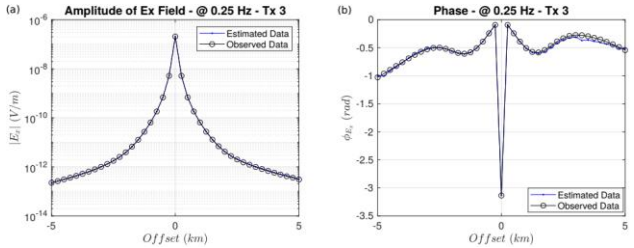

Figure 10 *- Graph of comparison between observed (black curve) and estimated (blue curve) MCSEM data of transmitter 3 for the frequency of 0.25 Hz. (a) Amplitude of the electric field; (b) Phase of the electric field using total variation regularization.*

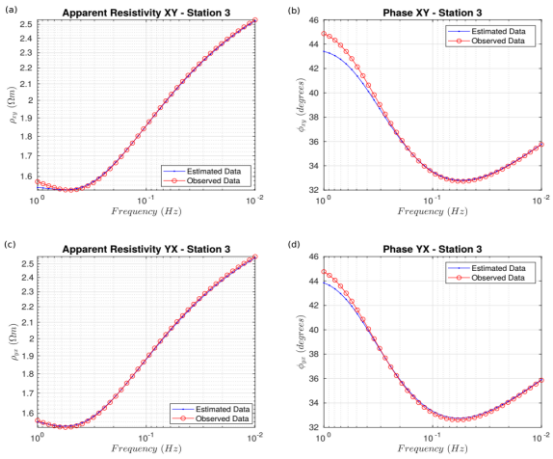

Figure 11 *- Graph of comparison between observed (red curve) and estimated (blue curve) MMT data of the receiver 3. (a) Apparent resistivity XY; (b) Phase XY; (c) Apparent resistivity YX; (d) Phase YX using total variation regularization.*

Conclusions

The experiment shows us the effectiveness of the joint inversion when we observed a great improvement in the estimated model by this inversion.

Acknowledgments

Ours special thanks go to Petrobras for the financial incentive through the research project. We also thank all the authors who helped to develop this work.

References

ABUBAKAR, A., M. LI, G. PAN, J. LIU, AND T. HABASHY 2011, Joint mt and csem data inversion using a multiplicative cost function approach: *Geophysics*, 76, F203-F214.

ASTER, R. C., B. BORCHERS, AND C. H. THURBER, 2018, Parameter estimation and inverse problems*: Elsevier*.

ANDRÉIS, D., AND L. MCGREGOR, 2008, Controlled-source eletromagnetic souding in shallow water: Principles and applications: *Geophysics*, 37, F21-F32.

BORTOLOZO, C. A., 2016, Inversão conjunta 1d e 2d de dados de eletrorresistividade e tdem aplicados em estudos de hidrogeologia na bacia do paraná: PhD thesis, Tese de Doutorado (Geofísica), IAG-USP, São Paulo.

COMMER, M., AND G. A. NEWMAN, 2009, Three-dimensional controlled-source electromagnetic and magnetotelluric joint inversion: *Geophysical Journal International*, 178, 1305-1316.

CONSTABLE, S., AND C. J. WEISS, 2006, Mapping thin resistors and hydrocarbons with marine em methods: Insights from 1d modeling*: Geophysics*, 71, G43-G51.

CREPALDI, J. L., A. ZERILLI, T. LABRUZZO, G. B. DOS SANTOS, AND M. P. BUONORA, 2015, Inversão conjunta sísmica/em para sal alóctone: 14th International Congress of the Brazilian Geophysical Society & EXPOGEF, Rio de Janeiro, Brazil, 3-6 August 2015, *Brazilian Geophysical Society*, 190-193.

DA PIEDADE, A. A., 2020, Modelagem e inversão 3d de dados do método csem, incluindo efeito de polarização induzida: PHD thesis, Federal University of Pará, Brazil.

DA SILVA, H. F., 2018, Modelagem anisotrópica 3d de dados do método marinho de fonte eletromagnética controlada (mcsem 3d): PhD thesis, Tese de Doutorado (Geofísica), PPGGf-UFPA, Belém.

GRIBENKO, A. V., AND M. S. ZHDANOV, 2011, Joint 3d inversion of marine csem and mt data, in SEG Technical Program Expanded Abstracts 2011: *Society of Exploration Geophysicists*, 552-556.

HANSEN, P. C., 2005, Rank-deficient and discrete ill-posed problems: numerical aspects of linear inversion*: Siam*, 4.

HEINCKE, B., M. JEGEN, AND R. HOBBS, 2006, Joint inversion of mt, gravity and seismic data applied to sub-basalt imaging, in SEG Technical Program Expanded Abstracts 2006*: Society of Exploration Geophysicists*, 784-789.

MACKIE, R., M. D. WATTS, AND W. RODI, 2007, Joint 3d inversion of marine csem and mt data, in SEG Technical Program Expanded Abstracts 2007: *Society of Exploration Geophysicists*, 574-578.

MOJABI, P., AND J. LOVETRi, 2009, Overview and classification of some regularization techniques for the gauss-newton inversion method applied to inverse scattering problems: IEEE Transactions on Antennas and Propagation, 57, 2658-2665.

OLIVEIRA JR, V. C., AND L. UIEDA, 2014, Tópicos de inversão em geofísica.

RIJO, L., 2004, Eletrical geophysics 1-d earth modeling.

Silva, J. B., W. E. Medeiros, and V. C. Barbosa, 2001, Pitfalls in nonlinear inversion: *Pure and Applied Geophysics*, 158, 945-964.

SILVA, M. W. C., AND C. R. T. RÉGIS, 2017, Inversão tridimensional de dados mt e mcsem in-line e broadside: Technical report, UFPA/FADESP/PETROBRAS.

Simpson, F., and K. Bahr, 2005, Practical magnetotellurics: Cambridge University Press.

VOZOFF, K., AND D. JUPP, 1975, Joint inversion of geophysical data*: Geophysical Journal International*, 42, 977-991.

WIIK, T., K. HOKSTAD, B. URSIN, AND L. MÜTSCHARD, 2013, Joint contrast source inversion of marine magnetotelluric and controlled-source electromagnetic data: *Geophysics*, 78, E315-E327.

ZHANG, R., AND T. LI, 2019, Joint inversion of 2d gravity gradiometry and magnetotelluric data in mineral exploration: *Minerals*, 9, 541.

ZHDANOV, M. S., 2002, Geophysical inverse theory and regularization problems: *Elsevier*, 36.